Chapter 7

Holograms in Optical Wireless Communications

Mohammed T. Alresheedi,

Ahmed Taha Hussein and Jaafar M.H. Elmirghani

Additional information is available at the end of the chapter

http://dx.doi.org/10.5772/intechopen.68408

Abstract

Adaptive beam steering in optical wireless communication (OWC) system has been shown to offer performance enhancements over traditional OWC systems. However, an increase in the computational cost is incurred. In this chapter, we introduce a fast hologram selection technique to speed up the adaptation process. We propose a fast delay, angle and power adaptive holograms (FDAPA-Holograms) approach based on a divide and conquer methodology and evaluate it with angle diversity receivers in a mobile optical wireless (OW) system. The fast and efficient fully adaptive FDAPA-Holograms system can improve the receiver signal to noise ratio (SNR) and reduce the required time to estimate the position of the receiver. The adaptation techniques (angle, power and delay) offer a degree of freedom in the system design. The proposed system FDAPA-Holograms is able to achieve high data rate of 5 Gb/s with full mobility. Simulation results show that the proposed 5 Gb/s FDAPA-Holograms achieves around 13 dB SNR under mobility and under eye safety regulations. Furthermore, a fast divide and conquer search algorithm is introduced to find the optimum hologram as well as to reduce the computation time. The proposed system (FDAPA-Holograms) reduces the computation time required to find the best hologram location from 64 ms using conventional adaptive system to around 14 ms.

Keywords: adaptive hologram, delay spread, SNR

1. Introduction

In general, holography is the storage of the phase and amplitude information of a wavefront. It is usually used as an approach to create three-dimensional (3D) images of objects through interference between a wavefront diffracted and a coherent reference beam. In optical wireless communications (OWC), the hologram is a transparent or reflective device that is used to

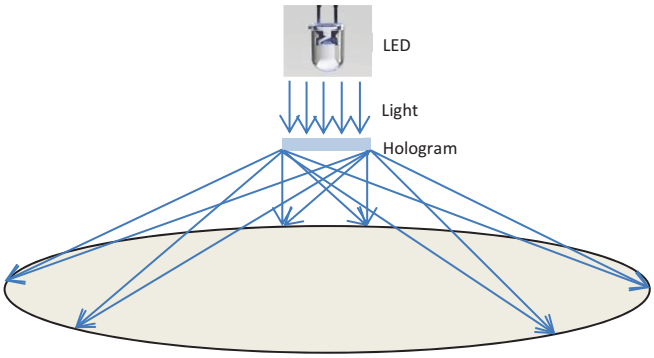

Figure 1. Holographic diffuser with uniform intensities that cover desired area.

spatially modulate the phase or amplitude of the energy passing through it. **Figure 1** illustrates the effect of a diffusing hologram on a set of rays from a light source. Here, the light source (light emitting diode (LED)) is split into a number of beams that cover the desired area.

Holograms can be produced from mathematical description or physical object. In mathematical approach, any wavefront can be generated. If mathematical method is implemented with a computer, the hologram is called a computer generated hologram (CGH). A ground glass diffuser can be given as a simple example of physical object diffuser, where ground glass can be placed at the output of a laser to change it from a point source to a large area source. However, this type of hologram cannot be controlled.

Beam steering has been widely studied in wireless communication systems to maximise the signal to noise (SNR) at the receiver [1, 2]. It is also considered as an attractive option in optical wireless communication (OWC) systems to enhance the system performance [3, 4]. New adaptive technique using beam steering is introduced in visible light communication (VLC) links in Ref. [5]. The goal is to maximise the SNR at the receiver in all possible locations within an indoor environment. Simulations results have shown that high data rate up to 20 Gb/s can be achieved by partially steering some of the beams towards the receiver location. Multi-input-multi-output (MIMO) infrared (IR) links employing beam steering method has been introduced in Ref. [6]. Furthermore, demonstration of IR-linked energy transmission using beam forming along with a spatial light modulator (SLM) is shown in Ref. [7]. An efficient power and angle adaptation technique is proposed in Refs. [1–4] in order to help the IR optical wireless (IROW) transmitter to optimise the diffusing spots distribution. These methods (power and angle adaptations) are able to enhance the received signal strength level, regardless of the receiver's location, the receiver's field of view (FOV) and transmitter's position. A significant performance improvement using beam angle and beam power adaptation in a line strip multi-beam system (APA-LSMS) is shown in Refs. [1, 2]. However, a cost has to be paid due to the complex adaptation requirements. The adaptive APA-LSMS transmitter needs to generate a single spot and scanning with all the possible locations (around 8000 locations) in the room in order to find the receiver and then generate the hologram with optimum powers and angles. This makes APA-LSMS system design very challenging.

In this chapter, we aim to point out the impairments of IROW links and propose new efficient solutions beyond those reported in Refs. [1–4]. We report an adaptive hologram selection method employing simulated annealing (SA) to generate diffusing spots (multi-beam). The proposed system is pre-calculated and stored all the holograms in memory. Each stored hologram is suited for a given transmitter and receiver location. Hence, it eliminates the need to calculate holograms real time at each transmitter-receiver location. We model fast angle and power adaptive holograms (FAPA-Holograms) and fast delay, angle and power adaptive holograms (FDAPA-Holograms) mobile OW systems, in conjugation with angle diversity receivers [8]. The conventional diffuse system (CDS) and line strip multi-beam systems (LSMS) are studied for comparison purposes. The ultimate goal of the proposed systems: FAPA-Holograms and FDAPA-Holograms is to reduce the time required to generate hologram at optimum transmitter and receiver location as well as to enhance the overall system performance such as SNR and channel bandwidth in a typical indoor environment. A significant improvement can be obtained by increasing the scanned stored holograms in our systems to approach the original power and angle adaptive methods proposed previously in Refs. [1, 2]. However, increasing the number of scanned stored holograms leads to an increase in the computation time needed to find the best hologram. To overcome this issue, we introduce a divide and conquer (D&C) algorithm to select the best hologram among a finite vocabulary of holograms, hence speed up the adaptation process associated with these adaptive systems [8]. High data rates of 2.5 and 5 Gb/s are considered for the FAPA-Holograms and FDAPA-Holograms systems.

The remainder of this chapter is organised into the following sections: Section 2 presents The IROW room setup and channel characteristics. Section 3 presents the proposed systems' configurations. Section 4 introduces the simulation results and discussion of the IROW systems. Finally, conclusions are drawn in Section 5.

2. The IROW room setup and channel characteristics

In order to study the impact of directive ambient light noise sources and multipath dispersion, as well as their effect on the received data flow, consideration was given to an unoccupied rectangular room that had no furnishings, with dimensions of 8 m × 4 m × 3 m (length × width × height). Researchers in Ref. [9] have studied and investigated the power reflected in indoor IROW system. The study found that the light reflected on either ceiling or wall is Lambertian in nature (mode n = 1). They also found that the wall reflected power by 80% whereas ceiling by only 30%. In this chapter, we consider that the rays reflected from door and windows are similar to those coming from walls. The reflecting elements from walls and ceiling can be modelled by dividing the surfaces into a small square shape, which can operate as secondary Lambertian transmitter with n = 1.

The accuracy of the impulse response profile is controlled by the size of the reflecting elements. Therefore, element sizes of 5 cm × 5 cm for the first order reflections and 20 cm × 20 cm for the second order reflections are employed for all arrangements. Previous work studied the received optical power within an indoor environment. They found that most of the received optical power is located within the two first order reflections (1st and 2nd). Third order and

higher reflections are highly attenuated [10, 11]. Hence, two bounces are considered in our calculations. All the proposed systems use an upright transmitter with 1 W optical power. Furthermore, the significant signal to noise ratio (SNR) improvement of the hologram-proposed systems is used to reduce the transmit power to 80 mW reducing the power density on the adaptive hologram and helping eye safety.

In OW communication links, intensity modulation with direct detection (IM/DD) is considered the most viable approach. The indoor OW IM/DD channel can be fully specified by its impulse response $h(t)$, and it can be modelled as a baseband linear system given by

$$I(t, Az,\ El) = \sum_{m=1}^{M} Rx(t) \otimes h_m(t,\ Az,\ El) + \sum_{m=1}^{M} Rn(t,\ Az,\ El). \tag{1}$$

where $I(t, Az, El)$ is the current instantaneous due to m reflecting elements, El and Az are the directions of arrival in the elevation and azimuth angles, t is the absolute time, $x(t)$ is the optical power transmitted, $\otimes$ denotes convolution, M is the total number of receiving elements, R is the photodetector responsivity and $n(t, Az, El)$ is the background noise. The delay spread is a good tool to measure signal spread due to multipath propagation. The delay spread can be written as [12, 13]:

$$DS = \sqrt{\left(\sum_{\forall i} (t_i - \mu)^2 P_{r_i}^2\right) \Big/ \sum_{\forall i} P_{r_i}^2} \tag{2}$$

where the time delay t_i is associated with the received power P_{r_i} (P_{r_i} reflects the impulse response $h(t)$ behaviour) and μ is the mean delay given by

$$\mu = \sum_{\forall i} t_i P_{r_i}^2 \Big/ \sum_{\forall i} P_{r_i}^2. \tag{3}$$

The delay spared is deterministic for a given stationary transmitter-receiver and reflecting elements' positions. The delay spread can change for a given transmitter-receiver location when the reflecting elements moves or an object is entering and leaving the environment. However, the impact of such a change is not considered in this work and has not been investigated by other researchers.

The SNR of the received signal can be calculated by taking into account the powers associated with logic 0 and logic 1 (P_{S0} and P_{S1}), respectively. The SNR is given by [14]:

$$SNR = \left(\frac{R(P_{s1} - P_{s0})}{\sigma_0 + \sigma_1}\right)^2 \tag{4}$$

$$\sigma_0 = \sqrt{\sigma_{pr}^2 + \sigma_{bn}^2 + \sigma_{s0}^2} \text{ and } \sigma_1 = \sqrt{\sigma_{pr}^2 + \sigma_{bn}^2 + \sigma_{s1}^2} \tag{5}$$

where σ_{pr}^2 represents the receiver noise, which is a function of the design used for the preamplifier; σ_{bn}^2 represents the background shot noise component and σ_{s0}^2 and σ_{s1}^2 represent the shot

noise associated with the received signal (P_{S0} and P_{S1}), respectively. The signal-dependent noise (σ_{si}^2) is very small due to the weak received optical signal, see the experimental results reported in Ref. [15]. In this study, we used the PIN-FET transimpedance preamplifier proposed in Ref. [16]. The background shot noise calculations can be found in Ref. [3]. Nine branches angle diversity receiver is used to reduce the impact of multipath dispersion. In this work, we employed the non-imaging angle diversity receiver design proposed in Ref. [8]. We considered maximum ratio combining (MRC) scheme. Calculations of MRC method can be found in our previous work in Refs. [1, 19].

In order to consider the impact of background noise, we use eight light bulbs in the room. These lights are used for illuminations. However, in OW receiver, the signals arrived from each light are considered as undesired signals which can be modelled as background shot noise. In this study, we assumed that Philips PAR 38 Economic' (PAR38) was used as spotlight in which each unit of light radiates 65 W within a narrow beam width. The light from these units can be modelled as a Lambertian radiant intensity with order nl = 33.1 [11]. Additional simulation parameters are given in **Table 1**.

3. Proposed systems' configurations

A CDS and non-adaptive LSMS are two widely studied configurations in the literature; therefore, they are modelled and used for comparison purposes in order to evaluate the improvements offered through the proposed configurations. More information about CDS and LSMS system can be found in Refs. [9–11].

3.1. FAPA-hologram

Power adaptation and beam angle can be considered as an effective approach, which helps to have an optimum power allocation and distribution of the diffusing spots. A single spot is produced by the adaptive transmitter to scan the ceiling and walls at approximately 8000 possible locations (2.86° beam angle increment [3]) in order to identify the best location. A liquid crystal device (IR hologram) is used to change the spot location at each step. Power adaptation technique can be used with angle adaptation to further enhance signal to noise ratio. The transmitter switches spots one by one and the receiver calculates the SNR (weight) associated with each spot. Then the feedback signal is sent by receiver at a low data rate to inform the transmitter about the SNR associated with each spot. The transmitter re-distributes the power among the spots based on their SNR weights [1] .The transmitter generates the hologram after finding optimum angles and power levels of spots. Intensive calculations and time are required from a digital signal processor (DSP). An adaptation approach is proposed where a finite vocabulary of stored holograms is used in order to get rid of computing the holograms at each step to identify the best location. The ceiling is divided into 80 regions (0.4 m × 1m per region), see **Figure 2**. This large number of regions has been selected based on our recent optimisation in Ref. [17].

Parameter	Configuration								
Width	4 m								
Height	3 m								
ρ x z wall	0.8								
y-z wall	0.8								
x-z op wall	0.8								
y-z op wall	0.8								
Floor	0.3								
	Transmitter								
Quantity				1					
Location (x,y,z)	(1 m, 1 m, 1 m)						(2 m, 7 m,1 m)		
Elevation				90°					
Azimuth				0°					
	Receiver								
Quantity	9								
Photodetector's area	10 mm^z								
Acceptance semi-angle	12°								
Location (x, y, z)	(1,1,1),(1,2,1),(1,3,1,),(1,4,1),(1,5,1),(1,6,1),(1,7,1)								
Elevation	90°	65°	65°	65°	65°	65°	65°	65°	65°
Azimuth	0°	0°	45°	90°	135°	180°	225°	270°	315°
	Resolution								
Time bin duration			0.5 ns				0.01 ns		
Bounces			1				2		
Surface elements			32,000				2000		
Number-of-spot lamps					8				
Locations				(1,1,1), (1,3,1), (1,5,1), (1,7,1) (3,1,1), (3,3,1), (3,5,1), (3,7,1)					
Wavelength					850 nm				
Preamplifier design	PIN-BJT						PIN-FET		
Bandwidth (BW)	50 MHz				2.5 GHz				5 GHz
Bit rate	50 Mbit/s				2.5 Gbit/s				5 Gbit/s

Table 1. Parameters used in simulation.

Holograms generated by means of a computer can produce spots with any prescribed amplitude and phase distribution. For FAPA-Holograms, all the spots have different weights (powers) and different phases. CGHs have many useful properties. Spot distributions can be computed on the

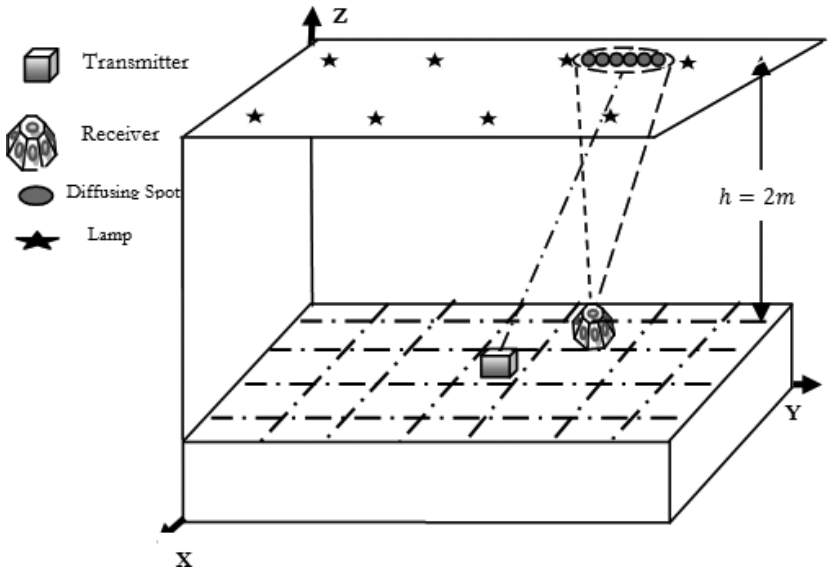

Figure 2. OW communication architecture of FAPA-Hologram system.

basis of diffraction theory and encoded into a hologram. Calculating a CGH means the calculation of its complex transmittance. The transmittance is expressed as follows:

$$H(u,v) = A(v,u).exp[j\phi(u,v)] \tag{6}$$

where $H(u, v)$ is complex transmittance function, $A(u, v)$ and $\phi(u, v)$ are amplitude and phase distribution, respectively. The parameters (u, v) are coordinates in the frequency space. The phase of incoming wavefront is modulated by hologram, whereas the transmittance amplitude is equal to unity. The analysis used in Refs. [18–20] has been employed for the design of the CGHs. The hologram $H(u, v)$ is considered to be in the frequency domain and the observed diffraction pattern $h(x, y)$ in the spatial domain. They are related by the continuous Fourier transform:

$$h(x,y) = \iint H(u,v)exp[-i2\pi(ux+vy)]dudv \tag{7}$$

The diffraction pattern of the hologram when it is placed in the frequency plane is given by

$$h(x,y) = RSsinc(Rx,Sy)\sum_{k=-\frac{M}{2}}^{\frac{M}{2}-1}\sum_{l=-\frac{N}{2}}^{\frac{N}{2}-1} H_{kl}exp[i2\pi(Rkx+Syl)] \tag{8}$$

where $sinc(a,b) = sin(\pi a)\ sin(\pi b)/\pi^2 ab$. The complex amplitude of the spots is proportional to some value of interest. But, the reconstruction will be in error because of the finite resolution of the output device and the complex transmittance of the resulting hologram. This error can be

considered to be a cost function. Simulated annealing (SA) is used to minimise the cost function [21]. The phases and amplitudes of every spot are determined by the hologram pixel pattern and are given by its Fourier transform. The constraints considered in the hologram plane are to discretise the phase from 0 *to* 2π and a constant unit amplitude for the phase only CGH.

Let the desired spots in the far field be $f(x, y) = |f(x, y)|\exp(i\varphi(x, y))$. The main target is to find the CGH distribution $g(v, u)$ that produces optimum reconstruction $g(x, y)$ that is very close to the desired distribution $f(x, y)$. The cost function (CF) is defined as a mean squared error which can be interpreted as the difference between the normalised desired object energy $f''(x, y)$ and the scaled reconstruction energy $g''(x,y)$:

$$CF_k = \sqrt{\sum_{i=1}^{M} \sum_{j=1}^{N} \left(|f''(i,j)|^2 - |g''_k(i,j)|^2 \right)^2}, \tag{9}$$

where $f''(x, y)$ represents the normalised desired object energy and $g''_k(i,j)$ represents the scaled reconstruction energy of the k^{th} iteration. Simulated annealing was used to optimise the phase of the holograms offline in order to minimise the cost function. The simulating annealing algorithm can help jump from local optima to close to a global optimum (minimising the cost function close to zero). The transition out of a local minima to global one is accomplished by accepting hologram phases that increase the mean squared error of the reconstruction with a given probability. The probability of accepting these phases is $exp(-\Delta CF/T)$, where $\Delta CF$is the change in error and T is a control parameter (the temperature of the annealing process). First, we start with a high value of T so that all the change in the hologram phases are accepted and then slowly lower T at each iteration until the number of accepted changes is small. This method is similar to melting a metal at a high value of T and then reducing the T slowly until the metal crystals freezes at a minimum energy. The changes of hologram phases relate to a small perturbation of the physical system, and the resulting change in the mean squared error of the reconstruction corresponds to the resulting change in the energy of the system. Therefore, this technique finds a hologram configuration, which has a minimum mean squared error (CF). For phase only CGHs, the constraints are constant amplitude and a random phase distribution φ_0 ($M \times N$). In the first iteration, a random phase is applied to help in the convergence of the algorithm.

For a large room of 8 m × 4 m, the floor is divided into 80 regions. A library that contains 6400 holograms is optimised offline using SA. In order to accurately identify the receiver location, a large number of holograms are required [17]. The optimum diffusing spots were pre-calculated based on the power and angle techniques shown in Ref. [1]. A total of 80 holograms are stored in a library and allocated for each region, the transmitter should cover the 80 possible receiver positions in the room, which means 6400 holograms are required to cover the entire room. The total number of holograms required is N^2, where N represents the number of regions into which the floor/ceiling is divided. **Figure 2** illustrates one hologram when the receiver is present at (1 m, 6 m and 1 m) and the transmitter is placed in the middle of room at (2 m, 4 m and 1 m). SA is used to optimise the phase of the CGH. **Figure 3** shows

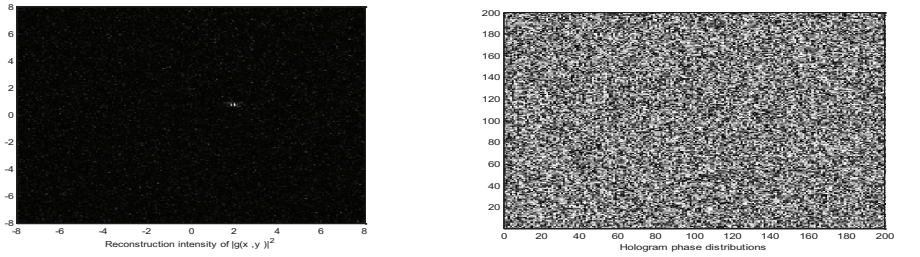

Iteration 1

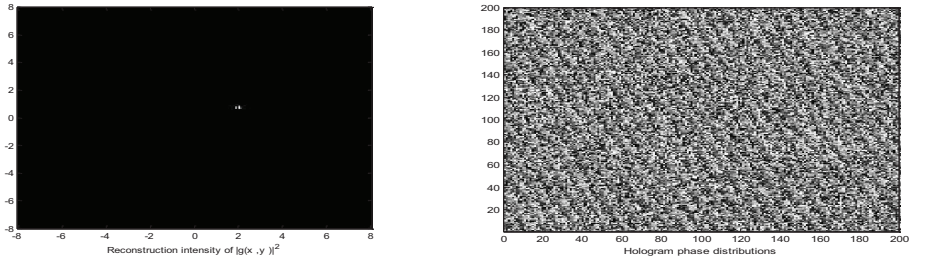

Iteration 5

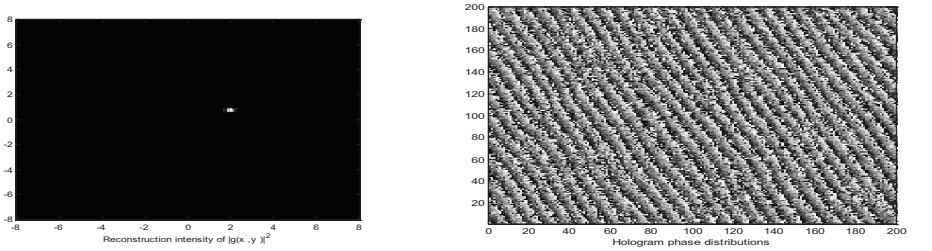

Iteration 15

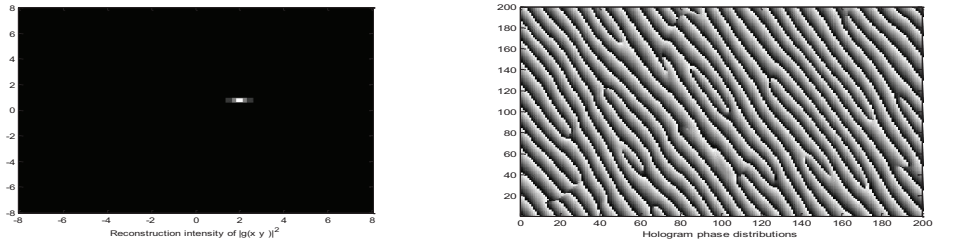

Iteration 100

Figure 3. The reconstruction intensity at the far field and hologram phase pattern at iterations 1, 5, 15, and 100 using simulated annealing optimisation. Different grey levels represent different phase levels ranging from 0 (black) to 2π (white).

phase distributions and hologram reconstruction intensity at the far field in four snapshots. When the number of iterations increases, the reconstruction intensities are improved. The desired spot intensity in the far field is shown in **Figure 4**. **Figure 5** shows the number of iterations versus cost function.

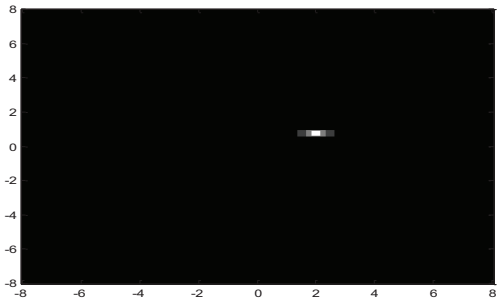

Figure 4. The desired spots intensity in the far field.

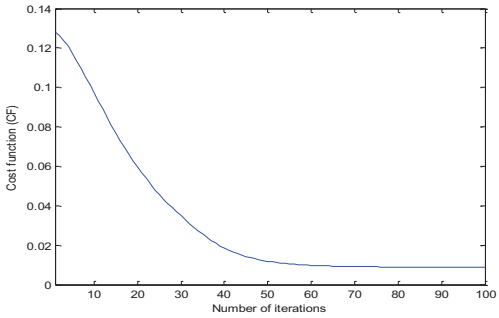

Figure 5. Cost function versus the number of iterations.

Scanning 6400 stored holograms in the system required a full search among all stored holograms, in order to select the best hologram. However, high complexity in term of the computation time is introduced. To solve this issue, a fast search technique is proposed to enhance the SNR via selecting the best hologram while reducing the computational time. The proposed search technique is based on a divide and conquer (D&C) method. Using the D&C algorithm, the transmitter is able to select the best hologram that can achieve the optimum receiver SNR. The fast search algorithm of our proposed system is applied for a single transmitter/receiver scenario as follows:

1. The stored holograms in the transmitter are first divided into four quadrants based on their transmission angles. The transmission angles associated with each quadrant are δ_{max-x} to δ_{min-x} and δ_{max-y} to δ_{min-y} in the x-axis and y-axis, respectively.
2. A single middle hologram is used in each group (quadrant) in order to find the first sub-optimum hologram.

3. The receiver calculates the SNR for each hologram and sends a pilot signal at low rate (feedback channel) to inform the transmitter about the SNR associated with each scanned hologram.

4. The transmitter selects the hologram that achieves the best SNR and identifies the new optimal quadrant (first sub-optimum quadrant) for next iteration.

5. The transmitter divides the sub-optimum quadrant into four sub-quadrants and applies steps 2–4 in order to find the second sub-optimal quadrant.

6. The D&C process is carried out and steps 2–5 are repeated to find the best location that has the highest SNR level at the receiver.

The proposed system reduces the computation time from 64 ms (each hologram required 1 ms to scan) taken by the classic beam steering system to 13 ms (13 possible locations should be scanned in all iterations $\times$ 1 ms).

3.2. FDAPA-hologram

To additionally enhance the performance of the IROW system, we introduce beam delay adaptation technique coupled with beam angle and power adaptation using hologram selection approach. The delay spread in a multi-beam spot IROW system is influenced by the spots' numbers and locations seen by each detector's FOV [3]. Therefore, switching all the beams simultaneously can introduce a differential delay between the neighbouring signals received at the receiver, hence spreading the pulse and limiting the 3-dB channel bandwidth. Instead of transmitting all the beams simultaneously, the delay adaptation algorithm sends the signal that has the longest journey first, and then sends the other signals with different differential delays (Δt) so that all the signals reach the receiver at the same time. A total of 10 μs time delay computation is carried out for each beam [8]. Therefore, a total of 1ms delay adaptation time is required for a beam. Our FDAPA-Hologram (delay, power and angle methods) requires only 14 ms adaptation time in order to select the best hologram. Assume the receiver initiates the adaptation every 1 s. This time is associated with a pedestrian speed of 1 m/s. Therefore, employing FDAPA-Hologram with a total 14 ms adaptation time introduces only 1.4%. Array element delayed switching is used to implement the delay adaptation method. The delay adaptation algorithm is explained as follows:

1. A transmitter first switches only the first beam (spot).

2. The receiver estimates the mean delay (μ) associated with first beam in the branch.

3. The receiver calculates the mean delay for all other branches.

4. The transmitter repeats steps 1–3 for other beams.

5. The receiver sends a feedback channel to update the transmitter about the delay associated with each beam.

6. The transmitter calculates the delay difference (Δt) between the beams as follows:

$$\Delta t_i = \max(t_{i\_max}) - t_i \; 1 \leq i \leq N_{spot} \tag{10}$$

7. The transmitter sends the beams with different times associated with their differential delay estimated in Eq. (10) to help the beam arrive at the receiver at the same time

The differential delay depends on the distances among the beams. If all the beams touch each other on the ceiling, then the differential delay will be few nano seconds, hence requiring timing control to switch such a beam within the required time.

4. Simulation results and discussion

In this section, we evaluate the performance of the proposed support systems in an empty room in the presence of multipath dispersion, receiver noise, back ground noise (light units) and mobility. The results are presented in terms of delay spread and SNR.

4.1. Delay spread

The delay spread of our adaptive proposed systems (FAPA-Holograms and FDAPA-Holograms) compared with CDS and LSMS system is shown in **Figure 6**. The results are presented when the transmitter is located near the room corner while the receiver moves along x = 2 m. The conventional pure diffuse system (CDS) has the largest delay compared with other systems. This is due to the diffuse transmission along with wide FOV at the receiver. Moreover, the delay spread of non-adaptive system LSMS is increased as the distance between the transmitter and receiver increases. The delay spread is almost independent of the distance between the transmitter-receiver in our hologram configurations, FAPA-Holograms and FDAPA-Hologram. This is due to beam angle adaptation technique where the proposed systems choose the hologram that has the best SNR. A significant reduction in the delay spread to 0.04 ns is achieved in our FAPA-Hologram system. Moreover, our delay adaptation method in FDAPA-Hologram reduces the delay spread of FDPA-Hologram by factor of 8. This improvement enhances the 3 dB channel bandwidth and increases the SNR at high transmission rates.

4.2. SNR

The SNR results of our proposed systems are shown in **Figure 7**. The proposed systems are tested under the influence of background noise and transmitter/receiver mobility. The proposed adaptive holograms are compared with conventional CDS and multi-beam angle diversity LSMS system to facilitate the results with previous work published in Refs. [9–11]. The results are shown when transmitters operate at 50 Mb/s. High data rates of 2.5 and 5 Gb/s will be also considered in the next section. The transmitter is located near the room corner while the receiver moves 1 m step along x = 1 m and x = 2 m. The LSMS system provides better results than CDS with wide FOV receiver. This is due to providing direct link though spots and using non-imaging angle diversity receiver. Although the improvement has been achieved, there is

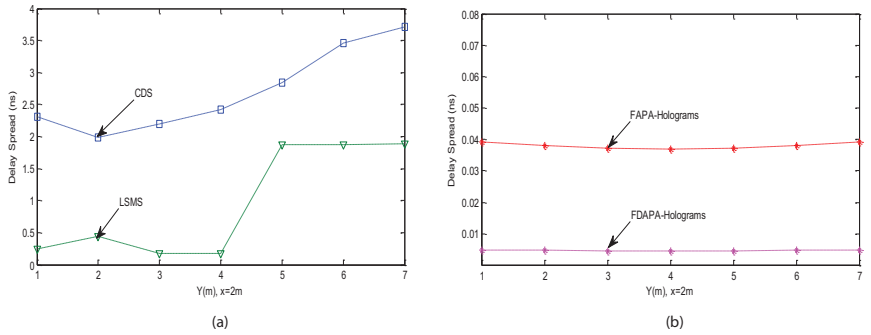

Figure 6. Delay spread of four configurations (a) CDS and LSMS, (b) FAPA-Holograms and APA-LSMS with angle diversity receiver, when the transmitter is placed at (1 m, 1 m, 1 m) and the receiver moves along $x = 2$ m line.

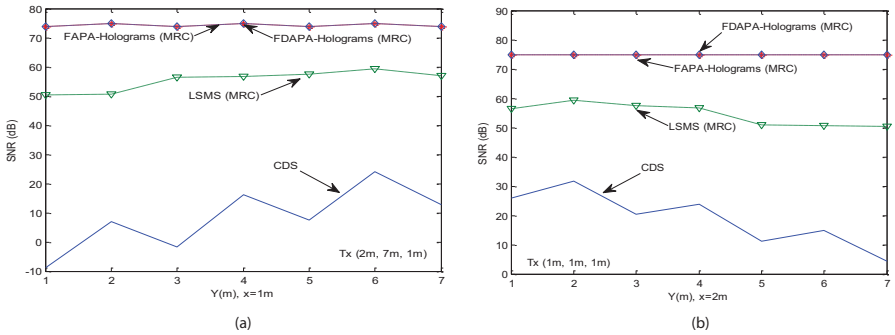

Figure 7. SNR of OW CDS, LSMS, FAPA-Holograms and FDAPA-Hologram at 50 Mbit/s, when the transmitter is located at (2 m, 7 m, 1 m) and (1 m, 1 m, 1 m) and the receiver mobiles along $x = 1$ m and $x = 2$ m lines.

degradation in the SNR results as LSMS transmitter move away from the receiver. For example, this is observed when the transmitter is moved towards the edge or the corner of the room at (2 m, 7 m and 1 m) and (1 m, 1 m and 1 m) while the receiver moves along $x = 1$ m and $x = 2$ m lines, respectively, as seen in **Figure 7(a)** and **(b)**. In order to overcome this significant reduction as well as improve the system performance, fast adaptive hologram (FAPA-Hologram and FDAPA-Hologram) systems are employed. Our proposed FAPA-Hologram achieves around 24 dB over the traditional LSMS system; see **Figure 7(b)**.

4.3. High data rate mobile IROW system

The results of the SNR achieved with our proposed FAPA-Hologram and FDAPA-Hologram allow the systems to reduce the total optical power transmit while operating at high data rates of 2.5 and 5 Gb/s. At high data rates, we considered a small photodetector area of 10 mm^2, in order to reduce the impact of high capacitance and improving receiver bandwidth. To the best of our knowledge, commercial photodetectors with a 10 mm^2 area and operating at high data rate are not common. However, researchers in Refs. [16, 22] have shown that the use of a small

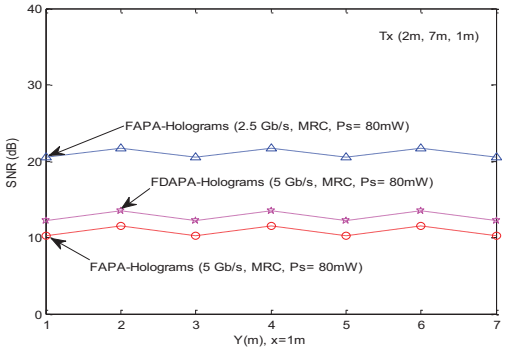

Figure 8. The SNR of proposed FDAPA-Holograms and FAPA-Hologram systems when operated at 2.5 and 5Gb/s, with a total transmit power of 80 mW.

detector area reduces the impact of high capacitance. In large commercial area, high speed detectors are starting to be used in free space optical systems. For example, Ref. [23] indicates that areas as large as 10 mm^2 and rise time as low as 10 ps are starting to emerge; however, the combination of large areas and fast response remains a challenge in photodetectors design. A 1 mW per beam is used to address the eye safety requirement in our proposed systems. Furthermore, we limit the power adaptation method where each beam cannot increase the power beyond 0.5 mW. The beams travel from the transmitter as group and spread until it reaches the object (reach to the ceiling in our case). At 10 cm distance each beam travel with different angle which can help in eye safety where the human eye cannot see more than one beam at time. Therefore, we propose that the transmitter is contained within a 10 cm deep enclosure to ensure that the human eye cannot be placed next to the transmitter. This can be achieved for example by placing the transmitter at the bottom of a laptop back cover (screen) and letting the beams emerge from the top of the back cover (screen). The proposed FAPA-Hologram achieves 20.5 dB at 2.5 Gb/s, see **Figure 8**. Moreover, at 5 Gb/s, the proposed FDAPA-Hologram offers around 2 dB SNR improvement over the FAPA-Hologram. This improvement is due to the use of beam delay adaptation method which helps to reduce the delay spread and improve 3dB channel bandwidth, hence increasing the SNR at the receiver. In terms of practical implementation, it should be noted that the diffraction limit has to be considered when considering commercially available spatial light modulators as the smallest pixel size that can be manufactured and operating wavelength to determine the maximum range of angles over which the beam can be steered [24]. This warrants further study.

5. Conclusions

The performance evaluation of the conventional CDS and non-adaptive LSMS can be significantly degraded by the transmitter/receiver mobility. In this chapter, the finite adaptive hologram using beam angle, power and delay adaptation techniques is introduced. All holograms are stored and pre-calculated in our adaptive system. A fast search algorithm based on the divide and conquer is reported. The fast algorithm reduced the time needed to generate

hologram to select the best stored hologram in the system. The adaptive proposed system is combined with an angle diversity receiver. Nine beaches non-imaging angle diversity receiver was used to further improve the received optical signal in the presence of background noise and transmitter mobility. At 50 Mb/s, our simulation results show that the adaptive FAPA-Holograms system provides around 35 dB SNR gain over non-imaging diversity LSMS system. The proposed FAPA-Holograms system using beam angle and power adaptation methods is able to guide the spots nearer to the receiver location at each given transmitter-receiver location. The angles and powers associated with each hologram stored in the system are pre-calculated without adding any complexity at the transmitter to recomputed holograms. In order to further improve system performance and reduce the effect of multipath dispersion, beam delay adaptation method coupled was introduced when the system operated at high data rates. The proposed FDAPA-Holograms system was examined under eye safety regulations. A total transmit power of 80 mW was used. The SNR results of our 5 Gb/s FDAPA-Holograms system were around 13 dB, under the impact of mobility as well as background noise. A fast search algorithm based on the divide and conquer was proposed to reduce the time needed to generate a real hologram and select the best stored hologram in the system.

Acknowledgements

The authors extend their appreciation to the International Scientific Partnership Program ISPP at King Saud University for funding this research work through ISPP# 0093.

Author details

Mohammed T. Alresheedi[1]*, Ahmed Taha Hussein[2] and Jaafar M.H. Elmirghani[2]

*Address all correspondence to: malresheedi@ksu.edu.sa

1 Department of Electrical Engineering, King Saud University, Riyadh, Saudi Arabia

2 School of Electronic and Electrical Engineering, University of Leeds, Leeds, UK

References

[1] Alresheedi MT, Elmirghani JMH. Performance evaluation of 5 Gbit/s and 10 Gbit/s mobile optical wireless systems employing beam angle and power adaptation with diversity receivers. IEEE Journal on Selected Areas in Communications. 2011;**29**(6):1328-1340. DOI: 10.1109/JSAC.2011.110620

[2] Alsaadi FE, Elmirghani JMH. High-speed spot diffusing mobile optical wireless system employing beam angle and power adaptation and imaging receivers. Journal of Lightwave Technology. 2010. **28**(16):2191-2206. DOI: 10.1109/JLT.2010.2042140

[3] Alresheedi MT, Elmirghani JMH. 10 Gbit/s indoor optical wireless systems employing beam delay, angle and power adaptation methods with imaging detection. IEEE Journal of Lightwave Technology. 2012;**30**(12):1843-1856. DOI: 10.1109/JLT.2012.2190970

[4] Alsaadi FE, Alhartomi MA, Elmirghani JMH. Fast and efficient adaptation algorithms for multi-gigabit wireless infrared systems. Journal of Lightwave Technology. 2013;**31** (23):3735-3751. DOI: 10.1109/JLT.2013.2286743

[5] Hussein AT, Alresheedi MT, Elmirghani JMH. 20 Gbps mobile indoor visible light communication system employing beam steering and computer generated holograms. Journal of Lightwave Technology. 2015;**33**(24):5242-5260. DOI: 10.1109/JLT.2015.2495165

[6] Wu L, Zhang Z, Liu H. Transmit beamforming for MIMO optical wireless communication systems. Wireless Personal Communications. 2014;**78**(1):615-628. DOI: 10.1007/s11277-014-1774-3

[7] Kim S, Kim S. Wireless optical energy transmission using optical beamforming. Optical Engineering. 2013;2(4):205-210. DOI: 10.1117/1.OE.52.4.043205

[8] Alresheedi MT, Elmirghani JMH. Hologram selection in realistic indoor optical wireless systems with angle diversity receivers. IEEE Journal on Optical and Networking (JOCN). 2015;**7**(8):797-813. DOI: 10.1364/JOCN.7.000797

[9] Gfeller FR, Bapst UH. Wireless in-house data communication via diffuse infrared radiation. Proceedings of the IEEE. 1979;**67**(11):1474-1486.DOI: 10.1109/PROC.1979.11508

[10] Kahn JM, Barry JR. Wireless infrared communications. Proceedings of the IEEE. 1997;**85** (2):265-298

[11] AI-Ghamdi AG, Elmirghani JMH. Line strip spot-diffusing transmitter configuration for optical wireless systems influenced by background noise and multipath dispersion. IEEE Transactions on Communications. 2004;**52**(1):37-45. DOI: 10.1109/TCOMM.2003.822160

[12] Yun G, Kavehrad M. Spot diffusing and fly-eye receivers for indoor infrared wireless communications. In: Proceedings 1992 IEEE Conference. Selected Topics in Wireless Communications; Vancouver, BC, Canada; 1992. pp. 286-292 DOI: 10.1109/ICWC.1992.200761

[13] Fadlullah J, Kavehrad M. Indoor high-bandwidth optical wireless links for sensor networks. Journal of Lightwave Technology. 2010;**28**:3086-3094. DOI: 10.1109/JLT.2010.2076775

[14] Desurvire E. Erbium-Doped Fiber Amplifiers: Principles and Applications. New York; A Wiley-Interscience Publication; 1994, ISBN: 978-0-471-58977-8

[15] Moreira A, Valadas R, Duarte AO. Optical interference produced by artificial light. Wireless Networks. 1997;**3**(2):131-140. DOI: 10.1023/A:1019140814049

[16] Leskovar B. Optical receivers for wide band data transmission systems. IEEE Transactions on Nuclear Science. 1989;**36(**1):787-793. DOI: 10.1109/23.34550

[17] Alresheedi MT, Elmirghani JMH. High-speed indoor optical wireless links employing fast angle and power adaptive computer-generated holograms with imaging receivers. IEEE Transactions on Communications. 2016;**64**:1699-1710. DOI: 10.1109/TCOMM.2016.2519415

[18] Jivkova S, Kavehard M. Multispot diffusing configuration for wireless infrared access. IEEE Transactions on Communications. 2000;**48**(6):970-978. DOI: 10.1109/26.848558

[19] Seldowitz MA, Allebach JP, Sweeney DE. Synthesis of digital holograms by direct binary search. Applied Optics. 1987;**26**:2788-2798. DOI: org/10.1364/AO.26.002788

[20] Ramirez FA. Holography—Different Fields of Application. InTech. 2011. p. 158. ISBN 978-953-307-635-5. DOI: 10.5772/750

[21] Carnevali P, Coletti L, Patarnello S. Image processing by simulated annealing. IBM Journal of Research and Development. 1985;**29**(6):569-579

[22] Elmirghani JMH, Chan HH, Cryan RA. Sensitivity evaluation of optical wireless PPM systems utilizing PIN-BJT receivers. IEE Proceedings—Optoelectronics. 1996;**143** (6):355-359. 10.1049/ip-opt:19960880

[23] Available from: http://www.cablefree.co.uk/faqs/pin-photodiodes-faqs/. [Accessed 20 June 2015]

[24] McManamon PF et al. A review of phased array steering for narrow-band electrooptical systems. Proceedings of the IEEE. 2009;**97**(6):1078-1096. DOI: 10.1109/JPROC.2009.2017218